

# An Overview of Experimental and Numerical Results on the Performance of Plasma Antennas Arrays

T.Anderson<sup>1</sup>, D.Melazzi<sup>2</sup>, A. D. J. Fernandez Olvera<sup>3</sup>, V.Lancellotti<sup>3</sup>

<sup>1</sup> Haleakala Research and Development Inc., Brookfield, MA, USA, [tedanderson@haleakala-research.com](mailto:tedanderson@haleakala-research.com)

<sup>2</sup> University of Padova, Padova, Italy, [davide.melazzi@gmail.com](mailto:davide.melazzi@gmail.com)

<sup>3</sup> Eindhoven University of Technology, Eindhoven, The Netherlands, [a.j.fernandez-olvera@student.tue.nl](mailto:a.j.fernandez-olvera@student.tue.nl), [v.lancellotti@tue.nl](mailto:v.lancellotti@tue.nl)

**Abstract**—Gaseous plasma antenna arrays (PAA) constitute a promising alternative to conventional metallic antennas for applications in which fast reconfigurability with respect to some property (e.g., the directivity) is desired. In this communication we give an account of the ongoing research on PAAs by presenting experimental and numerical results.

**Index Terms**—Antenna, plasma, measurement, simulation, reconfigurable, beam-forming, integral equations, Method of Moments, domain decomposition.

## I. INTRODUCTION

A Gaseous Plasma Antenna (GPA) consists of a plasma discharge confined in a dielectric tube. Since the plasma behaves as a conductor when 1) the tube is energized and 2) the discharge is driven at a frequency smaller than the plasma frequency, a GPA can transmit and receive electromagnetic (EM) waves [1] as a metallic antenna can. Plasma tubes used as radiators may come in different shapes (e.g., loops or monopoles), whereas the plasma can be generated through various methods depending on the intended application. Generation techniques include DC discharge, Radio-Frequency (RF) surface wave plasmas, and laser-initiated atmospheric discharges.

It has been concluded that the performance of a plasma antenna is similar to that of a copper wire antenna in every respect [1]. However, GPAs have many potential advantages over conventional metallic antennas [2], namely: (i) GPAs can be reconfigured with respect to frequency, gain and beam-width; (ii) they are reconfigurable electrically rather than mechanically on time scales the order of microseconds to milliseconds; (iii) they are transparent to incoming EM waves whose frequency is greater than the plasma frequency; (iv) as GPAs operating at different frequencies do not interfere with each other, they can be stacked to form complex plasma antenna arrays (PAA) [3], in which unused (i.e., turned-off) plasma elements are virtually transparent to EM waves.

A Smart Plasma Antenna (SPA) is an array of plasma antennas endowed with smart signal processing algorithms. In addition to the general advantages mentioned above, SPAs allow (i) identifying the direction of an incoming signal, (ii) tracking and locating the antenna beam on a mobile target, (iii) steering the beam in the direction of interest while minimizing interferences.

Various plasma systems have been proposed to meet different requirements. Borg *et al.* used surface waves to excite a plasma column which was intended as an RF

communication antenna [4]. Manheimer proposed a plasma reflector concept that relies on plasma reflector's agility and broad-band performance to replace phased arrays in radar systems [5]. Lastly, Grewal and Hanson proposed a solid-state plasma leaky-wave antenna in which beam scanning features are achieved by tuning the density of an optically induced plasma [6].

In this communication an account is given of the experimental and numerical analysis carried out by the Authors to investigate the performance of PAAs.

## II. EXPERIMENTAL ACTIVITY

We have considered the performance of a plasma reflector antenna (Figure 1) as compared to the behaviour of an antenna with similar design though comprised of a metallic reflector. The conventional metallic antenna was designed as an offset-fed cylindrical-parabolic reflector, and features a parabolic cylinder 71 cm high and 93 cm long. This is an offset configuration in which the parabolic sector is derived from a larger 132-cm-diameter dish. The focal distance of the parabola is 33 cm. The reflector is illuminated by a line source feed that is realized with a pillbox antenna. The latter, placed in front of the reflector antenna in the prime focal configuration, has a flared mouth to provide a nominal -10-dB-amplitude taper across the vertical dimension of the reflector. The pillbox feed is itself a parabola along the largest dimension. The focal distance of the pillbox parabola is 23 cm, and the depth of the pillbox (including the flare) is approximately 36 cm. The spacing of the feed parallel plates was chosen to allow the resulting horizontal polarization. The working frequency for the test was 3.0 GHz, which is well within the nominal bandwidth of the WR-284 waveguide used.



Figure 1 Practical example of plasma reflector antenna.

### A. The reconfigurable nature of the plasma reflector antenna

In conventional metallic antennas the conducting parts cannot be modified and are always present. By contrast, in GPAs the plasma can be extinguished and the antenna disappears. The two basic operation modes of a plasma antenna are plasma on and plasma extinguished (off). These are also the two basic modes of reconfiguration we have considered for the plasma reflector antenna of Figure 1. When the plasma reflector is on with the plasma frequency much greater than the frequency of the incident EM waves, the latter are reflected, but when the plasma is extinguished, the plasma reflector antenna becomes transparent. Other modes of reconfiguration are possible if the incident EM waves have a frequency much greater than the plasma frequency of one plasma antenna reflector but much less than the plasma frequency of another plasma antenna reflector. In this case the EM waves are transparent for the first plasma antenna reflector, but get reflected by the other. Still another mode of reconfiguration is possible with plasma reflector antennas if the plasma frequency varies from one plasma tube to the next. In this case we can obtain reconfigurable steering and focusing. This can be done in either the reflective or refractive mode. This is an important reconfiguration process for electronically steerable plasma satellite antennas that are conformal.

This same principle of reconfiguration applies to all types of GPAs. In PAAs, higher-frequency plasma antennas can transmit and receive through lower-density low-frequency plasma antennas. This enables GPAs with different plasma frequencies to be nested. Any number of these plasma antennas can be turned on or off to create a reconfigurable bandwidth or beamwidth.

### B. Pulsing techniques for ionization of gas to plasma inside plasma tubes

Experiments have been done to determine the best way to ionize the gas. For instance, plasma tubes can be ionized by means of DC current. However, provided that the tubes are ionized by extremely short bursts of DC current, then remarkable improvements can be achieved. In fact, the plasma is produced in an extremely short time of approximately 2 microseconds, and yet the plasma persists for a much longer time (~1/100 seconds). Consequently, if the pulsing rate is increased to 1 KHz, the tubes work at essentially constant density. There are three benefits to this new mode of operation. Firstly, the exciting current flows for only 2 microseconds, while it is off for one millisecond. As a result, the discharge current is only on for 0.2% of the time, so current-driven instabilities are not present for most of the time. In general, though, current-driven instabilities have been proven to be not problematic for GPAs. Moreover, operating the plasma tubes in the non-current-carrying, afterglow state will produce considerably less noise than what is produced in the current-carrying state. Nevertheless, we have found that even in the current-driven state the thermal noise in a GPA can be made less than that of a corresponding metal antenna.

This is true for operating frequencies above 1.27 GHz for a fluorescent tube and for lower frequencies if the pressure in the plasma fluorescent tube is reduced sufficiently. Secondly, the plasma density produced by means of the pulsed-power technique is considerably higher than the plasma density obtained with the same power supplied in the steady-state. This property has two beneficial consequences. The plasma antenna can operate at much higher plasma frequencies and densities as compared to the steady-state without destroying the discharge tube electrodes. Formerly, using commercial fluorescent tubes, we were limited to steady-state operation below 800 MHz because of the electrode design. Thanks to the pulsing technique, we can operate GPAs at several GHz and above. The upper frequency limit has not been explored. Finally, GPAs can work at much higher plasma frequencies and densities with lower average power consumption, because energy is only expended during the pulse.

### C. Results

The GPA in question (Figure 1) consists of an array of plasma tubes which play the role of the metallic reflector. The plasma reflector is comprised of 17 fluorescent light tubes, and the tube spacing was chosen so as to provide efficient operation at 3.0 GHz. The radiation patterns of the reference solid reflector and of the plasma reflector are shown in Figure 2; the patterns are very similar to each other with reduced sidelobe levels for the GPA. The plot of Figure 2 also shows the relative amplitude of the field scattered by the plasma antenna when the tubes are not energized; the scattered field (~20 dB below the maximum value during operation) is primarily due to reflections from the plasma containers and the electrodes. These experimental results are outstanding considering that the plasma reflector design was restricted to the usage of commercial off-the-shelf tubes.

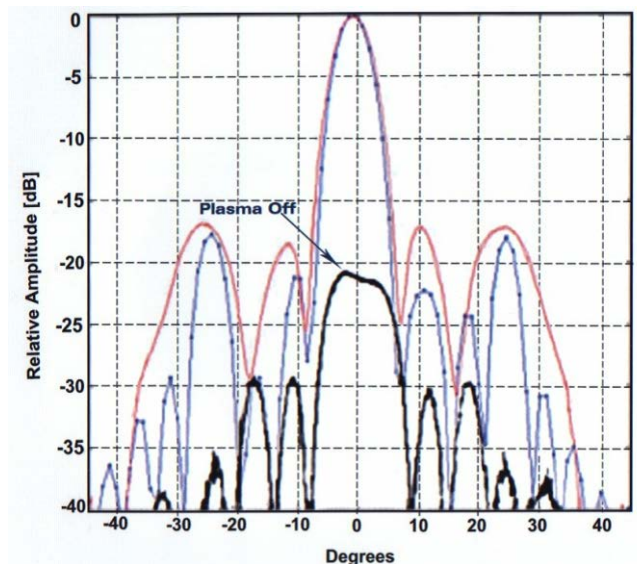


Figure 2 Radiation pattern of plasma reflector (line with blue dots), solid reflector (red solid line), and plasma reflector when the tubes are not energized (black solid line) at 24 cm focus.

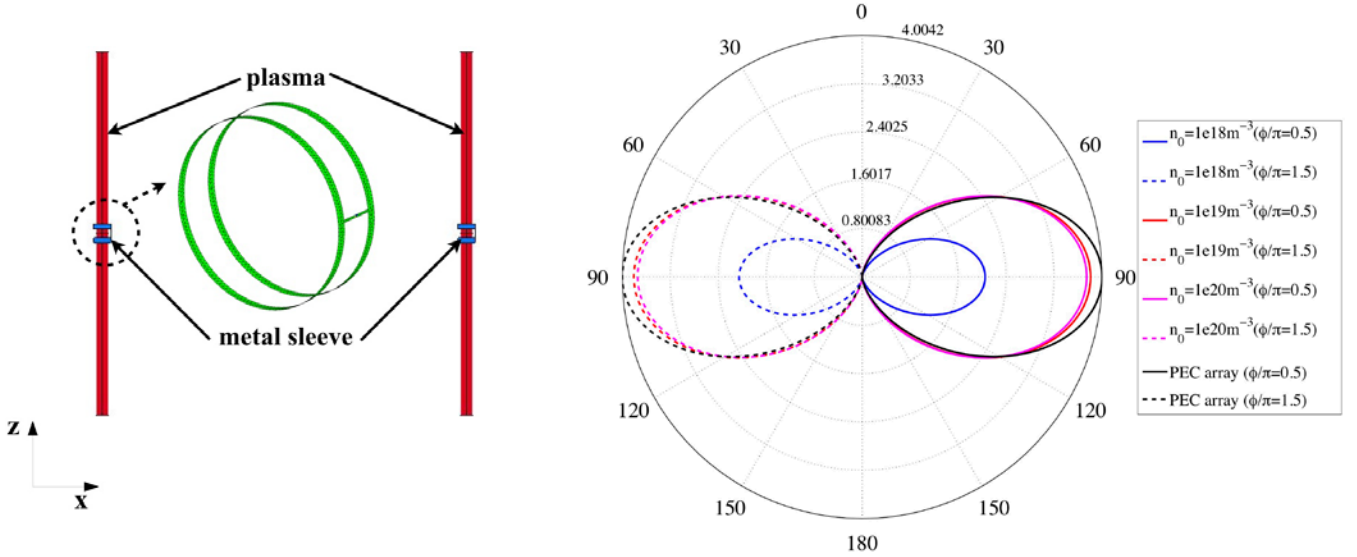


Figure 3 (Left) Model of the linear plasma array and close-up of the feeding metal-sleeve; (right) linear plasma array: antenna gain for a non-magnetized plasma driven at  $f = 2$  GHz, for different values of the uniform plasma density ( $n_0$ ), and compared to that of a PEC array of the same size.

### III. NUMERICAL ANALYSIS

The effect of the plasma parameters on radiation efficiency, reconfigurability and beam-forming of PAAs has been analysed in the frequency domain — time dependence in the form  $\exp(j\omega t)$  for fields and sources — with two numerical codes: ADAMANT [7] and LEGO [8]. In both codes, the plasma medium is modeled as a dielectric with dyadic permittivity; the plasma is assumed cold, weakly ionized, collisional, and magnetized. In a system of Cartesian coordinates with confining magneto-static field  $\vec{B}_0 = B_0 \hat{z}$ , the dyadic permittivity reads

$$\bar{\epsilon}_k = \epsilon_0 \begin{bmatrix} S & jD & 0 \\ -jD & S & 0 \\ 0 & 0 & P \end{bmatrix} \quad (1)$$

for  $k = 1, \dots, N_p$ , with  $N_p$  being the number of independent plasma regions that form the PAA, and  $\epsilon_0$  the permittivity of free space. Furthermore, the entries of  $\bar{\epsilon}_k$  have the following explicit expressions

$$S = 1 - \sum_{\xi} \frac{\omega_{p\xi}^2 (\omega - j\nu_{\xi})}{\omega [(\omega - j\nu_{\xi})^2 - \omega_{c\xi}^2]} \quad (2)$$

$$D = \sum_{\xi} \frac{\sigma_{\xi} \omega_{c\xi}}{\omega} \frac{\omega_{p\xi}^2}{\omega [(\omega - j\nu_{\xi})^2 - \omega_{c\xi}^2]} \quad (3)$$

$$P = 1 - \sum_{\xi} \frac{\omega_{p\xi}^2}{\omega [(\omega - j\nu_{\xi})^2]} \quad (4)$$

where  $\omega_{p\xi} \equiv (n_{\xi} q_{\xi}^2 / \epsilon_0 m_{\xi})^{1/2}$  is the plasma frequency,  $\omega_{c\xi} \equiv \sigma_{\xi} q_{\xi} B_0 / m_{\xi}$  is the gyrofrequency, with  $\sigma_{\xi}$  the particle charge sign, and  $\nu_{\xi}$  denotes the collision frequency. The subscript  $\xi$  refers to the index of the plasma species. In

writing (1), we assume the permittivity to be a function of the position, and hence profiles of plasma density, magneto-static field, electron temperature, and neutral pressure can be included.

In the numerical experiments described below, we have considered two configurations: a linear array of two plasma cylindrical dipoles, hereinafter referred to as the *linear plasma array*, and a plasma antenna comprised of a PEC cylindrical dipole surrounded by several plasma discharges, hereinafter referred to as the *reconfigurable plasma array*.

We have evaluated the antenna performance in terms of the antenna gain function for both configurations as plasma discharge parameters, i.e., plasma density and magneto-static field, are varied.

#### A. Linear plasma array

The PAA shown in Figure 3 is a linear array of two centered cylindrical plasma dipoles; the radiating elements are immersed in free space with horizontal separation of 7.5 cm, and are aligned with the  $z$ -axis of a Cartesian system of coordinates. The plasma discharges are driven by two metal sleeves 0.375 cm high and with a diameter of 1.25 cm. The dipoles have length and diameter of 7.5 cm and 0.25 cm, and are excited in phase with 1 V at the frequency of 2.0 GHz.

In order to investigate the influence of plasma discharge parameters on the performance of this PAA, we have considered a non-magnetized Argon plasma discharge with uniform plasma density  $n_0$  in the range  $10^{18} - 10^{20} \text{ m}^{-3}$ . We have assumed a neutral background pressure of 15 mTorr, and an electron temperature of 3 eV. With these parameters the collision frequency  $\nu_{\xi}$  can be computed consistently. The PAA has been analyzed with ADAMANT [7]; in particular, we have computed the antenna gain function  $g(\theta, \phi)$  as a function of the plasma density. As is apparent from Figure 3, the gain can be controlled by adjusting the plasma density. As can be



expected, the shape of the gain function is similar to that of an equivalent metallic linear array modeled by two PEC dipoles. When the plasma density is larger than  $10^{18} \text{ m}^{-3}$  the maximum gain of the PAA is similar to that of the equivalent metallic array.

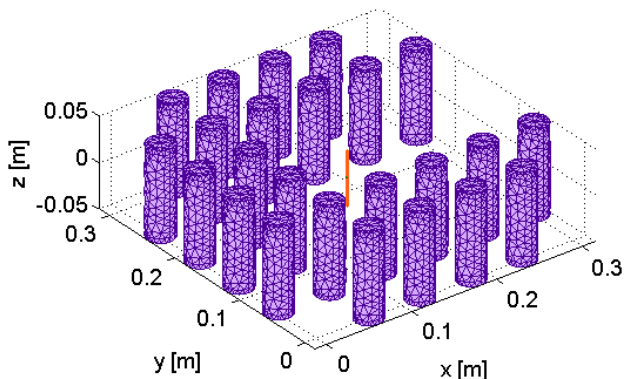


Figure 4 Reconfigurable PAA: model of the plasma tubes and the metallic dipole (only energized tubes are shown).

### B. Reconfigurable plasma antenna array

The reconfigurable PAA is shown in Figure 4. The radiating element is a metallic half-wavelength center-fed cylindrical dipole. The latter is surrounded by 24 plasma tubes arranged in a square lattice with unit cell of side 6 cm [3]. The dipole has length and radius of 6 cm and 0.1 cm, and it is excited with 1 V at the frequency of 2.27 GHz. The height and the diameter of a plasma tube are 10 cm and 3 cm, and the distance between the centers of two neighboring tubes is 6 cm.

An Argon plasma discharge with uniform density of  $10^{18} \text{ m}^{-3}$  is driven inside the tubes; the plasma is cold and weakly ionized with electron temperature of 3 eV and neutral background pressure 15 mTorr. Depending on which plasma tubes are off, the active tubes around the dipole realize a plasma waveguide of sorts which, for the configuration of Figure 4, is opened towards the positive  $x$ -direction. The PAA has been solved with LEGO [8]. Specifically, we have investigated the effect of an external magneto-static field ( $B_0$ ) on the beam-steering capability of the PAA, by varying the confining magneto-static field (aligned with the axes of the tubes) in the range from -0.1 T to 0.1 T.

The computed antenna gain function relative to the ideal isotropic radiator is plotted in Figure 5 as a function of  $\phi$  for  $\theta=90^\circ$ . As can be seen, the opening causes the PAA to radiate substantially toward the positive  $x$ -direction, whereas, by contrast, the gain of the dipole alone is independent of  $\phi$  and equal to  $\sim 1.6$ . This configuration can be rotated in steps of  $90^\circ$  in the  $xOy$  plane by selectively turning the plasma tubes on and off, thus allowing the main beam to be steered to alternatively to point in the four principal directions, and this provides reconfigurability of the antenna gain. Furthermore, it is worth noticing the tilting effect of the magneto-static field on the main lobe, namely, a positive  $B_0$  rotates the gain counterclockwise, while the opposite can be said for negative values. Conversely, for the values of  $B_0$  we have considered, no appreciable effect has been noticed on the maximum gain.

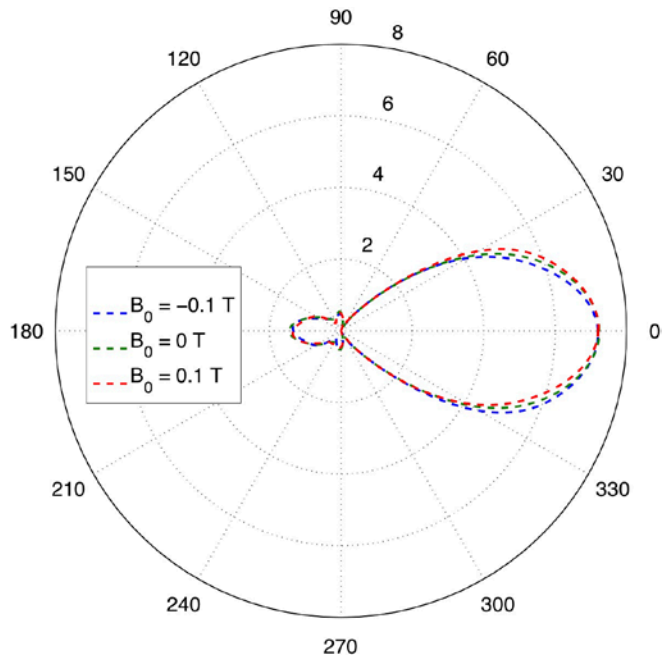


Figure 5 Reconfigurable PAA: effect of the magneto-static field ( $B_0$ ) on the antenna gain  $g(90^\circ, \phi)$  for the configuration of Figure 4.

## IV. CONCLUSIONS

We have shown that GPAs and PAAs can be a promising alternative to conventional metallic antennas in all those applications where fast reconfigurability is desired with respect to some antenna parameter, e.g., the gain function. Experimental research can benefit from numerical analysis in order to optimize the performance of PAAs by means of a suitable choice of plasma parameters, such as density or confining magneto-static field.

## REFERENCES

- [1] T. Anderson, *Plasma Antennas*. Artech House, ISBN:978-1-60807-144-9; 2011.
- [2] I. Alexeff, T. Anderson, *et al.*, "Experimental and theoretical results with plasma antennas," *IEEE Trans. Antennas Propag.*, vol. 32, no. 2, pp. 166-172, 2006.
- [3] A. D. J. Fernandez Olvera, D. Melazzi, V. Lancellotti, "Numerical analysis of reconfigurable plasma antenna arrays", *this conference*.
- [4] G.G. Borg, J.H. Harris, D.G. Miljak *et al.*, "Application fo plasma columns to radiofrequency antennas," *Appl. Phys. Lett.*, vol. 74, pp. 3272-3274, 1999.
- [5] W. Manheimer, "Plasma reflectors for electronic beam steering in radar systems," *IEEE Trans. Actions on Plasma Sci.*, vol. 19, n. 6, p. 1128, 2008.
- [6] G. Grewal and G.W. Hanson, "Optically-controlled solid-state plasma leaky-wave antenna," *Microwave Opt. Lett.*, vol. 39, pp. 450-453, 2003.
- [7] D. Melazzi, V. Lancellotti, "ADAMANT: A surface and volume integral-equation solver for the analysis and design of Helicon plasma sources," *Computer Physics Communications*, vol. 185, no. 7, pp. 1914-1925, 2014.
- [8] V. Lancellotti, D. Melazzi, "Hybrid LEGO-EFIE method applied to antenna problems comprised of anisotropic media," *Forum in Electromagnetic Research Methods and Application Technologies (FERMAT)*, 6, 2014, [www.e-fermat.org](http://www.e-fermat.org).